



## TESTING AN AXIAL FLOW FAN DESIGNED FOR AIR-COOLED STEAM CONDENSER APPLICATION

Sybrand J. VAN DER SPUY<sup>1</sup>, Theodore W. von BACKSTRÖM<sup>1</sup>, Detlev G. KRÖGER<sup>1</sup>, Phillipe R.P. BRUNEAU<sup>2</sup>

<sup>1</sup>*Department of Mechanical and Mechatronic Engineering, Stellenbosch University, Joubert Street, Stellenbosch, 7600, South Africa*

<sup>2</sup>*SASOL-Sastech, PDP Kruger Street, Secunda, 2302, South Africa*

### SUMMARY

The axial flow fans used in air-cooled steam condensers (ACSCs) may be subjected to distorted inlet flow conditions, which lead to a reduction in volume flow rate delivered by the fans. Two axial flow fans were designed that exhibited higher fan static efficiency values and a much steeper pressure versus volume flow rate curve than that of a comparative fan. Small diameter models of one of the new fans and the comparative fan were tested in the perimeter fan position in a multiple fan test facility. The multiple fan results showed that the new fan exhibited a much higher volumetric effectiveness than the comparative fan at high levels of inlet flow distortion.

### INTRODUCTION

Air-cooled steam condensers (ACSCs) and air-cooled heat exchangers (ACHEs) offer a substantial benefit to the power generation and process industry by virtue of the fact that they use air and not water as cooling medium. Air-cooled technology is particularly attractive in regions where cooling water is expensive or its availability is limited. South Africa currently has the world's largest direct dry-cooled power plant, Matimba, located at Lephalale in the Limpopo Province. Matimba has a total power generation capacity of 3990 MW(e) and operates 288, 9.1 m diameter axial flow fans<sup>1</sup>. The two new coal-fired power stations (Medupi and Kusile) currently being built in South Africa will also be of the direct dry-cooled type. Both the new power stations will consist of 6 x 794 MW(e) units<sup>1</sup>.

An ACSC may consist of a rectangular array of axial flow fans that supply cooling air to a large bank of heat exchangers (see Figure 1). The typical components of such a facility would include the fan platform<sup>①</sup>, the gearbox and motor combination<sup>②</sup>, the axial flow fan (with bell mouth)<sup>③</sup>, the platform support pillar, the A-frame heat exchanger (with finned tubes)<sup>④</sup> and the turbine exhaust steam duct<sup>⑤</sup>.

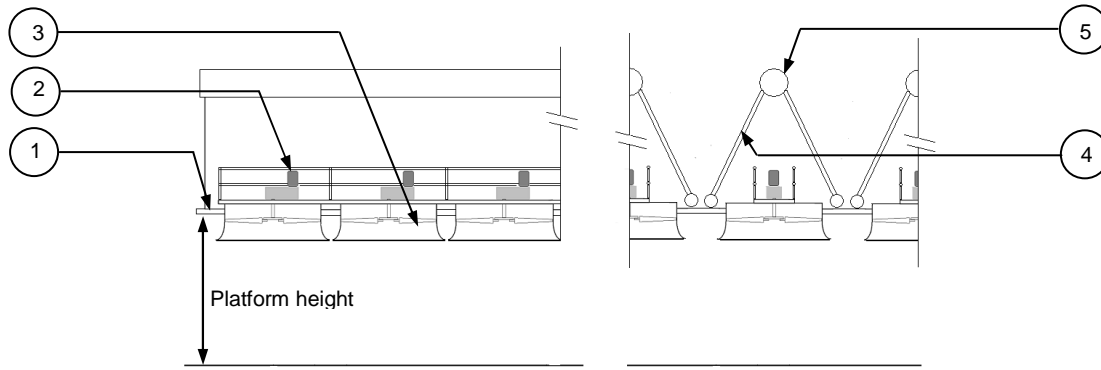


Figure 1: Sketch of typical A-frame air-cooled condenser<sup>1</sup>

Based on their location within the array, for instance around the perimeter, the fans may be subjected to distorted inlet flow conditions caused by cross flow upstream of the fan inlets. The distorted inlet conditions are exacerbated by wind and the presence of buildings<sup>2</sup>. Distorted inlet conditions lead to a reduction in the volume flow rate of air delivered by the fan. The heat transfer capacity of the ACSC is strongly dependent on the air volume flow rate. The distorted inlet conditions therefore lead to a reduction in the total condenser capacity and consequently a reduction in plant power output.

Venter<sup>3</sup> used a 1.5 m diameter scaled model of an industrial axial flow fan (referred to as the V-fan) to conduct a series of fan tests in a BS 848 part 1 type A test facility<sup>4</sup>. A schematic of the facility is shown in Figure 2.

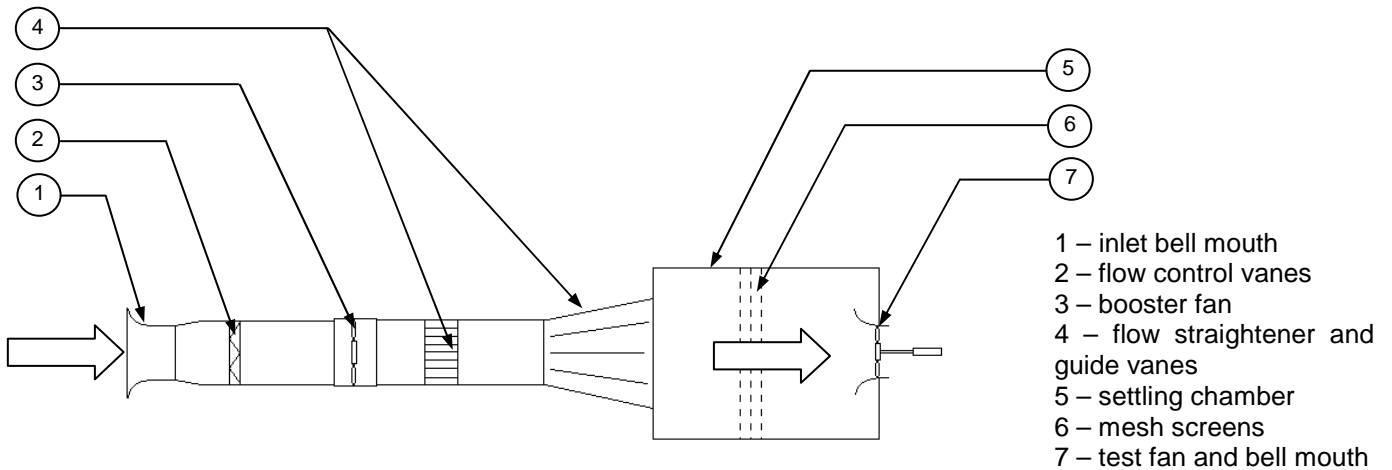


Figure 2: Schematic lay-out of BS 848 part 1 type A fan test facility.<sup>1</sup>

Venter evaluated the effect that auxiliary fan structures like support beams and inlet screens would have on the performance of the V-fan. He varied the fan blade tip clearance and derived a linear correlation between the increase in blade tip clearance and the corresponding reduction in fan static pressure and volume flow rate<sup>5</sup>. Venter also noticed the occurrence of reverse flow at the hub of the experimental fan and installed hub discs to increase the hub diameter of the fan rotor. Bruneau<sup>6</sup> designed a set of 1.542 m diameter axial flow fans, referred to as the B1- and B2-fans, to address the areas of concern associated with the V-fan. He optimized the hub-to-tip ratio of the fans for a specific operating point and used a “quadratic” swirl velocity distribution for the design of both sets

of fan blades<sup>7</sup>. The geometry and test results for the B-fans, as well as that of the V-fan, are discussed in the next section.

Salta and Kröger<sup>8</sup> conducted a set of experiments on a multiple fan test facility with a variable platform (or floor) height. Using the test results they were able to derive a correlation between platform height and fan system volumetric effectiveness ( $V/V_{ref}$ ) for the particular fans that were tested. The “volumetric effectiveness” represents the actual volume flow rate delivered by a multiple fan system, divided by the single fan, open inlet flow rate for the same number of fans. The fans that were tested as part of the investigation of Salta and Kröger may be termed “generic” and are not related to the B- or V-fans. Stinnes and von Backström<sup>9</sup> performed fan tests where they subjected the fans to set off-axis inlet flow angles ranging from 0° to 45°. For this purpose they used the BS 848 fan test facility shown in Figure 2 with angular inlet pipes between the settling chamber and the test fan. They evaluated the performance of both the B-fans and an S-fan (a replacement copy of the V-fan) and found that the fan power consumption and fan total-total pressure rise is independent of the angle of off-axis inflow.

Bredell et al.<sup>10</sup> conducted a set of computational fluid dynamics simulations using the actuator disc method where they evaluated the performance of a multiple fan installation using fan configurations similar to the B2- and V-fans. They found that fans having a steeper fan static pressure vs. volume flow rate characteristic are less susceptible to distorted inlet conditions and will subsequently experience a smaller reduction in volume flow rate through the fan than fans with a flatter static pressure characteristic. The results of Bredell et al. were confirmed by Van der Spuy et al.<sup>2</sup> who used the pressure jump method to obtain similar results for the same fans. These simulation results prompted an experimental investigation where scaled models of the B- and V-fans were tested in the perimeter fan position on a multiple fan test facility<sup>1, 11</sup>. These tests and their results are detailed in this document.

## AXIAL FLOW FANS

Two sets of axial flow fans formed part of this investigation. The first set, referred to as the V-fan and N-fan represented scaled models of a specific industrial fan. The second set, referred to as the B1- and B2-fan or B-fan, represented the fans designed by Bruneau<sup>7</sup>.

### V-fan and N-fan

These fans represent an existing industrial fan design. Very little information about these fans are available. The V-fan was a 1.542 m diameter, 8-bladed axial flow fan with a hub-to-tip ratio of 0.153 and adjustable rotor blade setting angles. The solidity of the V-fan at mid-span was 0.34, with a constant chord length of 0.12 m and tip clearance of 3 mm<sup>12</sup>. The N-fan was manufactured as a 0.63 m diameter scaled copy of the V-fan<sup>11</sup>. A picture of the N-fan is shown in Figure 3. The N-fan had a tip clearance of 2.5 mm<sup>11</sup>.

The industrial fan that is represented by this study forms part of a series of axial flow fan designs that covers a wide range of volume flow rates and fan pressures. It was therefore not designed for one specific operating point only.

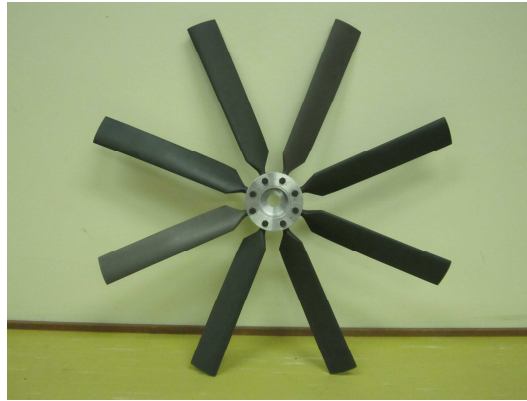


Figure 3: Photo of 0.63 m diameter N-fan.

### B1-, B2- and B-fan

The B1- and B2-fans were designed for a specific design point (210 Pa and 16 m<sup>3</sup>/s). The exact design procedure followed in the development of the B1- and B2-fans is addressed in a separate publication<sup>7</sup>. The format of the fans was constrained to be an 8-bladed rotor without stationary blade rows and rotor blades with adjustable blade setting angles. The hub-to-tip ratio and the solidity at mid-span of both fans were 0.4. The B1-fan blade section used a Clark-y profile, while the B2-fan blade section used a NASA LS-0413 profile. The tip clearance of the B1 and B2-fans was adjustable and for the purpose of the tests reported in this document it was set at 1.5 mm<sup>12</sup>.

A picture of the B-fan is shown in Figure 4. The B-fan was a 0.63 m diameter scaled copy of the B2-fan<sup>11</sup>. Compared to the low solidity tapered blade profile at the hub of the N-fan, the B-fan has a larger hub, with a well-defined blade-hub interface. The B-fan was designed with a tip clearance of 0.8 mm<sup>11</sup>.



Figure 4: Photo of 0.63 m diameter B-fan.

## SINGLE FAN TESTS

Individual performance tests for the V-, B1- and B2-fans were performed on a BS848 part 1 Type A fan test facility (see Figure 2). The tests were performed for an operating domain that straddles the design point mentioned previously. The values that were measured during the tests included the volume flow rate (using the bell mouth inlet), the static pressure in the settling chamber upstream of the fan, the fan shaft torque and the fan speed. The fan static pressure is given by:

$$p_{FS} = p_{amb} - (p_{static\ sett} + p_{dsett}) \quad (1)$$

where  $p_{FS}$  is the fan static pressure,  $p_{amb}$  is the ambient pressure,  $p_{static\ set}$  is the average absolute static pressure measured at the wall of the settling chamber upstream of the fan and  $p_{dsett}$  is the average dynamic pressure determined in the plane corresponding to the location of the static pressure measurements. Equation 1 corresponds to the equation for fan static pressure as given in BS848 part 1 for a type A test facility. The fan shaft power is given by:

$$P_{shaft} = \frac{2\pi NT}{60} \quad (2)$$

where  $N$  is the fan rotational speed,  $T$  is the fan shaft torque and  $P_{shaft}$  is the fan shaft power. The fan static efficiency is given by:

$$\eta_{FS} = \frac{p_{FS} V}{P_{shaft}} \quad (3)$$

where  $V$  is the volume flow rate of air passing through the fan. The volume flow rate is measured by means of a calibrated inlet bell mouth (item 1, Figure 2). Figure 5 shows the fan static pressure and fan static efficiency results for the V-fan (Stinnes<sup>12</sup>).

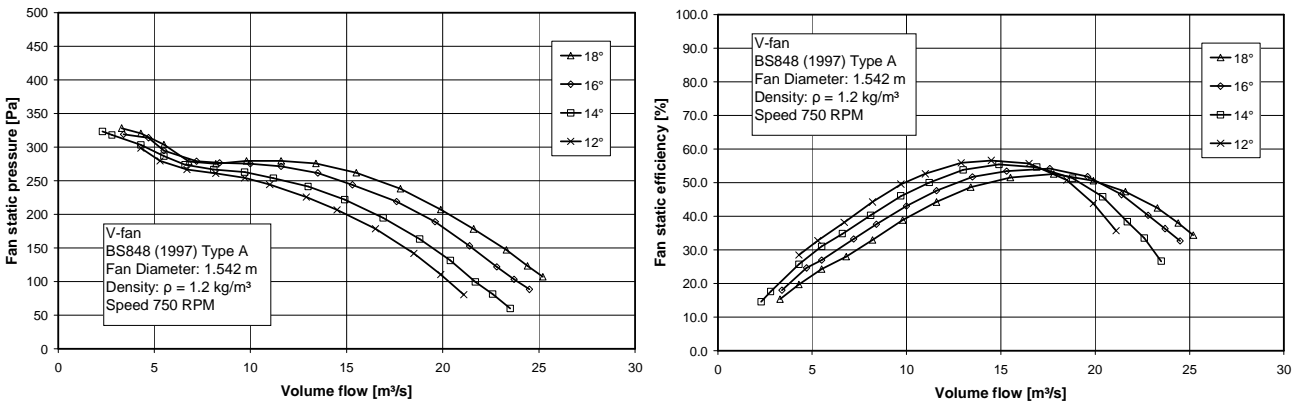


Figure 5: Fan static pressure (L) and fan static efficiency (R) for V-fan.

Figure 6 shows the fan static pressure and fan static efficiency results for the B1-fan (Stinnes<sup>12</sup>).

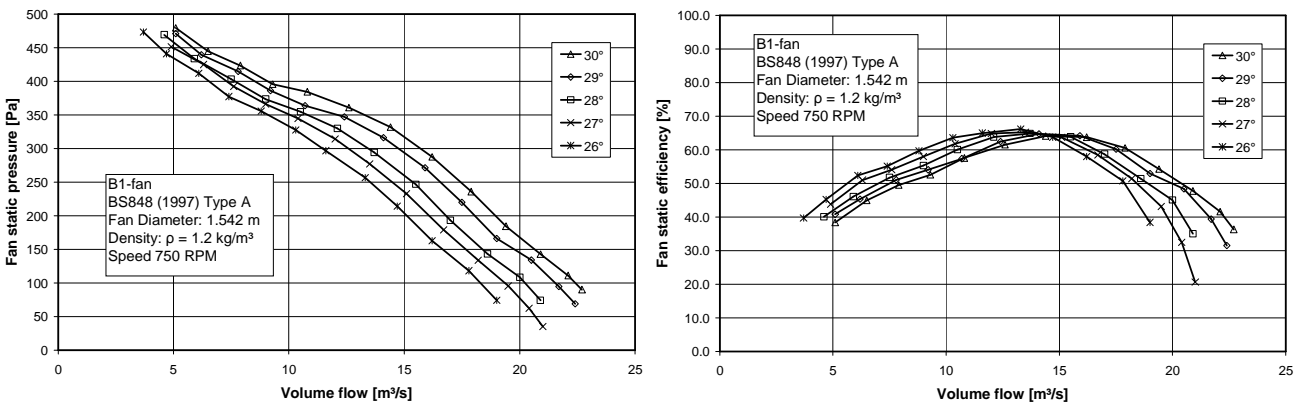


Figure 6: Fan static pressure (L) and fan static efficiency (R) for B1-fan.

Figure 7 shows the fan static pressure and fan static efficiency results for the B2-fan (Stinnes<sup>12</sup>).

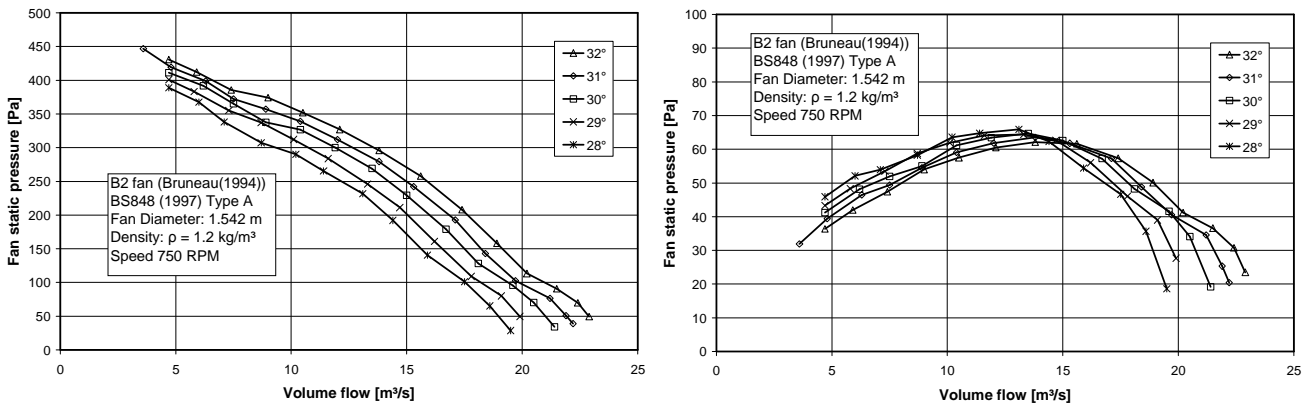


Figure 7: Fan static pressure (L) and fan static efficiency (R) for B2-fan.

Figure 8 shows a comparison of the fan static pressure and fan static efficiency results for the V-, B1- and B2-fan where they all pass through or close to an operating point of 210 Pa and 16 m<sup>3</sup>/s.

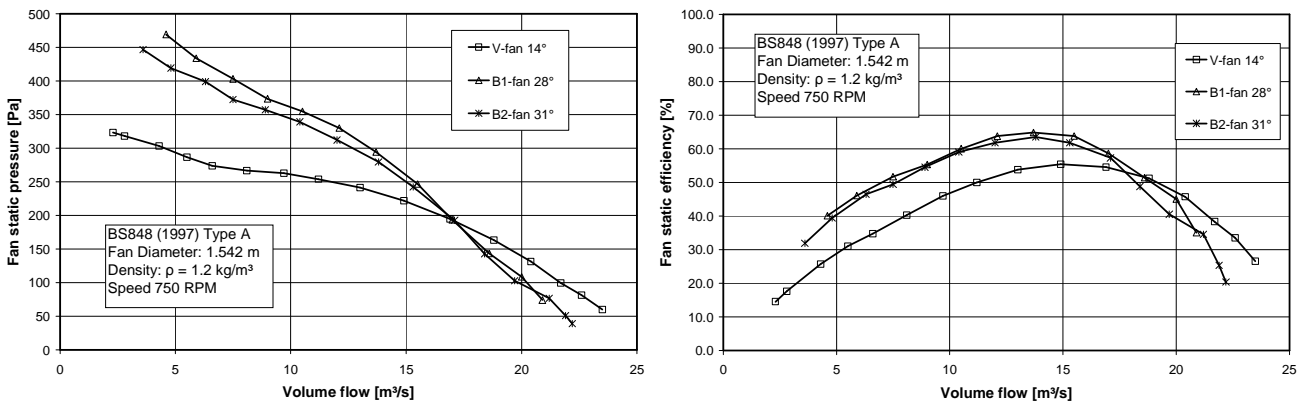


Figure 8: Fan static pressure (L) and fan static efficiency (R) for V-, B1- and B2-fan.

## MULTIPLE FAN TESTS

The B-fan and N-fan were tested in the perimeter (or edge) fan position in a multiple fan test facility<sup>1, 11</sup>. The facility consisted of three 630 mm diameter fans in parallel, extracting air from a common inlet chamber. Each of the three test fans was installed in a BS848 part 1 type B fan test tunnel<sup>11</sup>. Figure 9 shows a schematic lay-out of a single test tunnel. The volume flow rate was measured using a rotating vane anemometer, while the pressure was measured using four equally-spaced pressure taps downstream of the flow straightener. A torque transducer was installed in-line between the test fan and the electric motor. The physical size of the electric motor was set at 700 W to limit the flow obstruction caused by the motor. The limited power output of the electric motor meant that the tests on the multiple fan facility were performed at 1000 RPM.

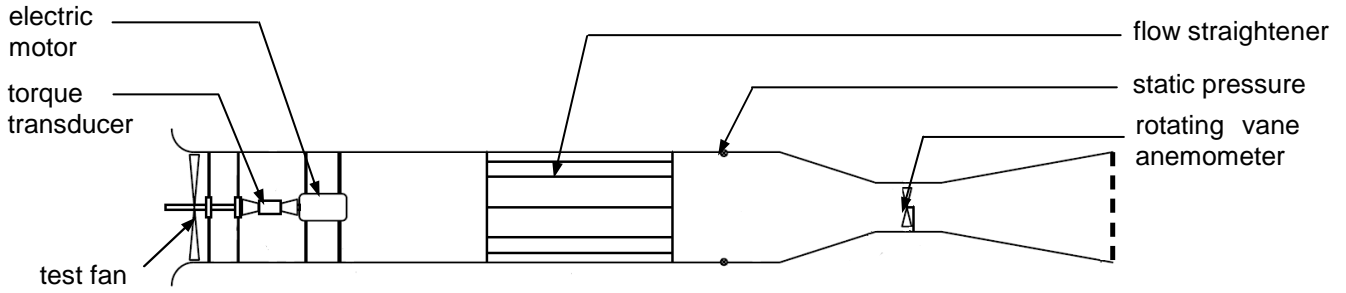


Figure 9: Schematic of 630 mm diameter fan tunnel for multiple fan facility<sup>11</sup>.

The 630 mm diameter test tunnel shown in Figure 9 was used to measure the fan performance curves of both the N- and B-fan. For this purpose, the test tunnel was fitted with a throttle at its outlet to vary the system resistance and thereby facilitate the measurements of fan characteristic curves at set blade angles. The fan curves were compared to those measured on the 1.542 m facility by scaling the results from the large facility down to that of the 630 mm facility using the fan scaling laws:

$$V' = V \left( \frac{N'}{N} \right) \quad (4)$$

$$p_{FS}' = p_{FS} \left( \frac{N'}{N} \right)^2 \left( \frac{\rho'}{\rho_{amb}} \right) \quad (5)$$

Figure 10 shows a comparison of the scaled 1.542 m fan test results and the 630 mm fan test results for the V-fan and the B-fan.

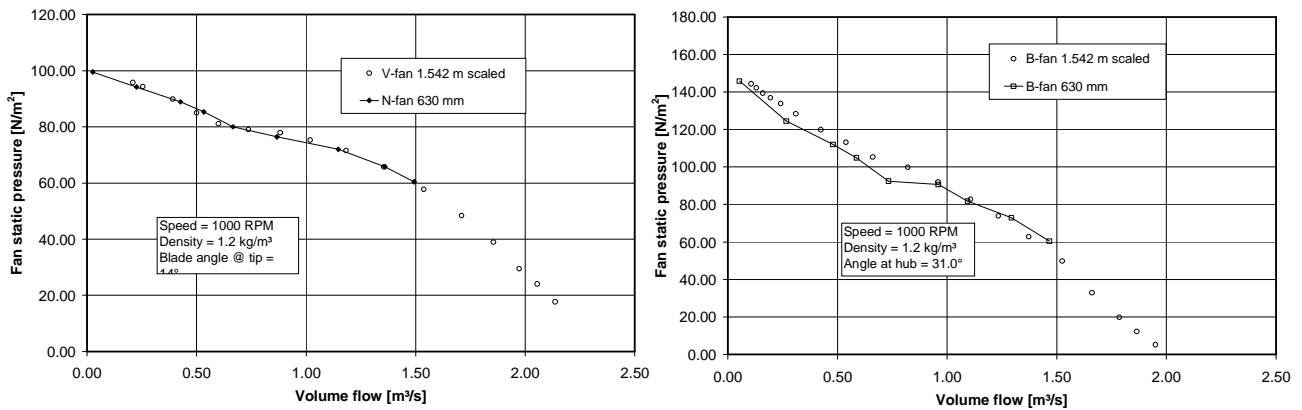


Figure 10: Comparison of large and small scale test results for V-fan (L) and B-fan (R).

The multiple fan facility was based on the facility used by Salta and Kröger<sup>8</sup> and was constructed in such a way that one of the three fans resembled a perimeter fan, while the format of the two inner fans was left unchanged. The floor height of the inlet chamber could be adjusted from fully open to a minimum height of 1.0 x fan diameter to vary the level of inlet distortion experienced by the perimeter fan. The side walls of the inlet chamber corresponded to the symmetry planes formed by the neighboring fans typically found in an ACSC. A schematic and photo of the multiple fan test facility is shown in Figure 11.

When considering the performance of an axial flow fan in an ACSC, the volume flow rate of air that it delivers is an indication of its ability to deliver the cooling medium required for condensation of the steam coming from the power generation turbines. The performance of a fan within a multiple fan installation is therefore reflected by its volumetric effectiveness<sup>8</sup>, defined as:

$$v_{oleff} = \frac{V}{V_{ref}} \quad (6)$$

where  $V$  is the volume flow rate passing through the fan under specific distorted inlet operating conditions and  $V_{ref}$  is the volume flow rate that would pass through the fan under single fan operating conditions with no distortion upstream of the fan inlet. Salta and Kröger<sup>8</sup> derived a correlation for the volumetric effectiveness of multiple fan system as follows:

$$\frac{V}{V_{ref}} = 0.985 - e^{-X} \quad (7)$$

where

$$X = \frac{(1 + 45/n_f)H}{d_f} \quad (8)$$

where  $n_f$  is the number of fans in a full fan row (in other words 6 for the above 3-fan facility),  $H$  is the floor height and  $d_f$  is the fan diameter.



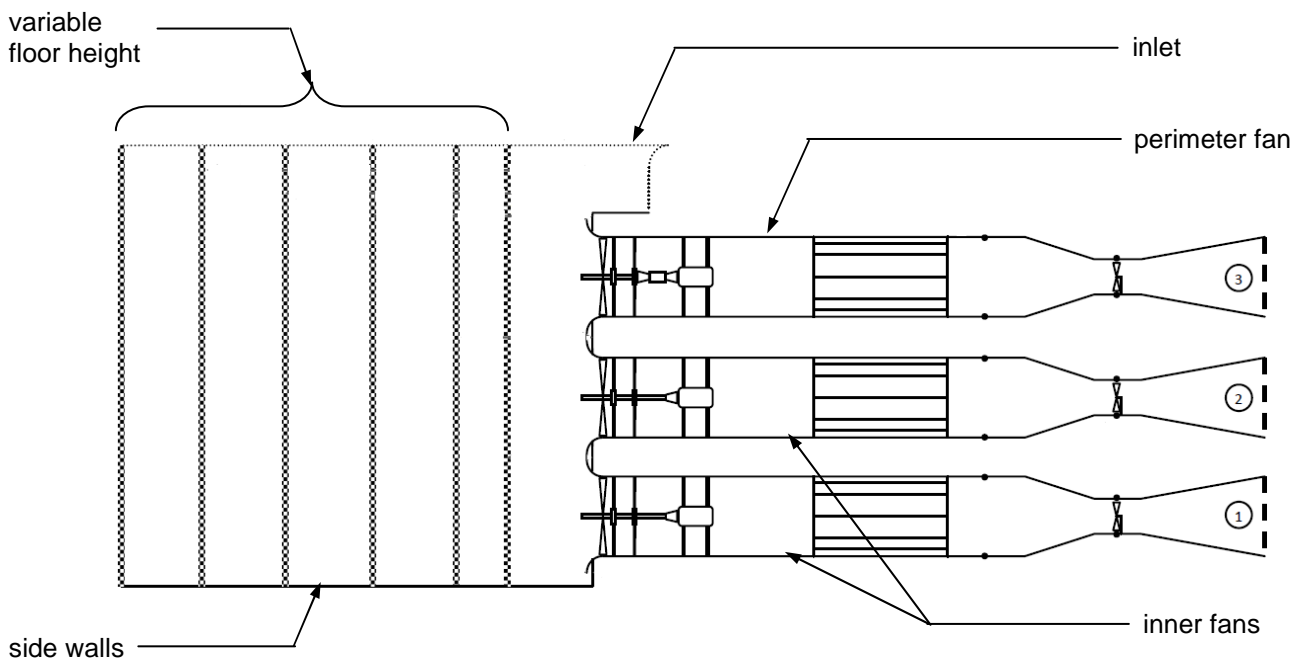


Figure 11: Schematic and photo of multiple fan facility<sup>11</sup>.

To investigate the performance of the N- and B-fan under distorted inlet conditions, the volumetric effectiveness of each of the fan configurations were measured in the perimeter fan position at different floor heights. During all the tests the N-fan configuration was used for the two inner fans. The throttle used previously to measure the system characteristic curve shown in Figure 10 was replaced with a fixed perforated resistance plate. Figure 12 shows a comparison of volumetric effectiveness between the correlation of Salta and Kröger<sup>8</sup> and those measured for the NNN- and BNN-system configurations<sup>11</sup>.

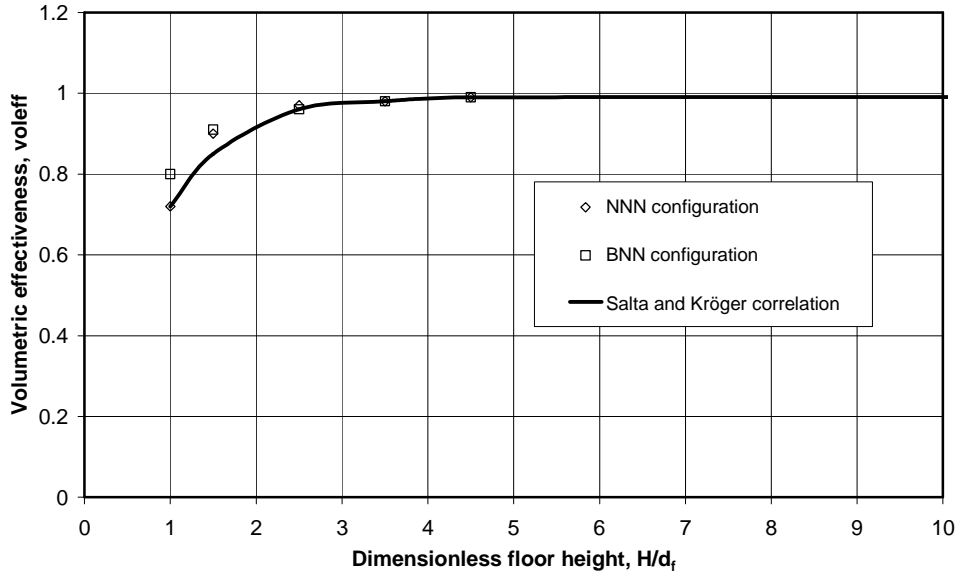


Figure 12: Comparison of system volumetric effectiveness.

Figure 13 shows a comparison of volumetric effectiveness between the B-fan and N-fan, when used in the perimeter fan position<sup>10</sup>.

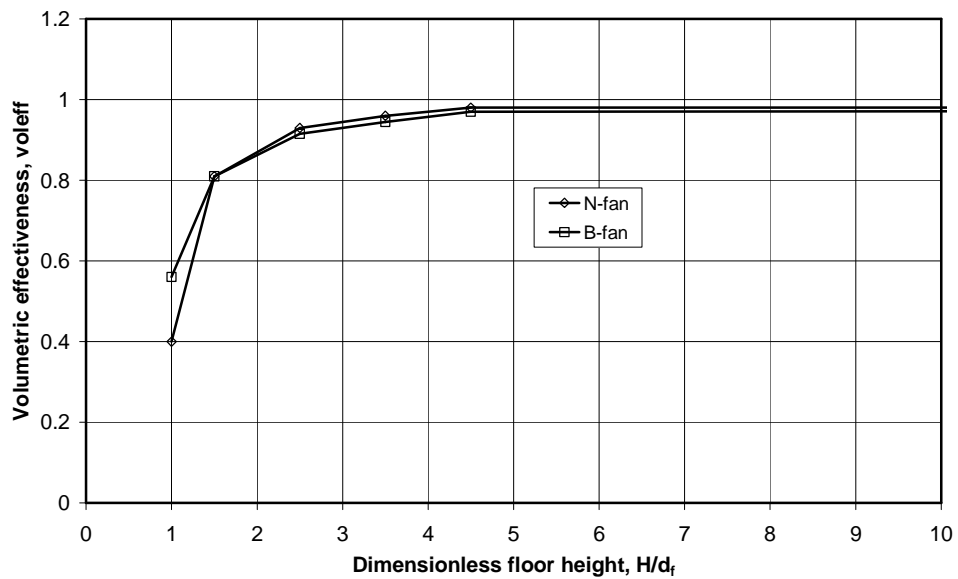


Figure 13: Comparison of edge fan volumetric effectiveness.

## DISCUSSION

Figure 8 shows that the B1- and B2-fans have similarly steep, static pressure characteristics, compared to the flatter characteristic of the V-fan. This can in principle be attributed to the higher average throughflow velocity of the B-fans, based on their larger hub diameter. The higher throughflow velocity means that the relative flow angle over the fan blade (and consequently the angle of attack over the blade) is more sensitive to a change in flow rate.

At the operating point, the static efficiency of both the B1- and B2-fans is in the order of 60%. As mentioned before, the B1- and B2 fans have the same hub-to-tip ratio and outlet velocity distribution. The only difference between the B1- and B2-fan is the choice of standard airfoil profile

that was used to design the fan blades, namely the Clark-y and NASA LS profiles. This explains the similarity in results obtained for the two fans.

The B-fans have a higher maximum fan static efficiency (62% and 60%) than the V-fan (54%). Venter<sup>3</sup> measured recirculation close to the hub of the V-fan at 16 m<sup>3</sup>/s. This can be attributed to the small hub-to-tip ratio and the low blade solidity of the V-fan close to the hub. The two B-fans on the other hand have an optimized hub-to-tip ratio, well-defined blade-hub interface and smaller tip clearance. The B-fan blades also have a generally better manufacturing finish on the fan blades than those of the V-fan. This would explain the higher efficiency of the two B-fans.

Figure 10 shows that the 630 mm diameter fans are representative of the 1.542 m diameter fans. This adheres to the requirement stated by Stinnes and von Backström<sup>9</sup> that when a scaled down fan is used to investigate multiple fan behaviour, its pressure characteristic curve should have the same slope as that of the fan that it represents. The multiple fan results showed that the B-fan and N-fan exhibited a similar volumetric effectiveness (0.98) at large floor heights. At the lowest floor height (1.0 x fan diameter) the volumetric effectiveness of the N-fan was however 0.4, compared to the volumetric effectiveness of the B-fan of 0.56. This correlates with the analysis results of Bredell et al.<sup>10</sup> and Van der Spuy et al.<sup>2</sup> who found that fans having a steeper fan static pressure vs. volume flow rate characteristic are less susceptible to distorted inlet conditions.

Van der Spuy<sup>1</sup> also measured the shaft power consumption of the B- and N-fans at different platform heights under similar conditions (see Figure 14). Van der Spuy<sup>1</sup> used a multiple fan facility that was similar to the one described in this document, except for replacing the flow straightener detailed in Figure 9 with a dummy plenum chamber.

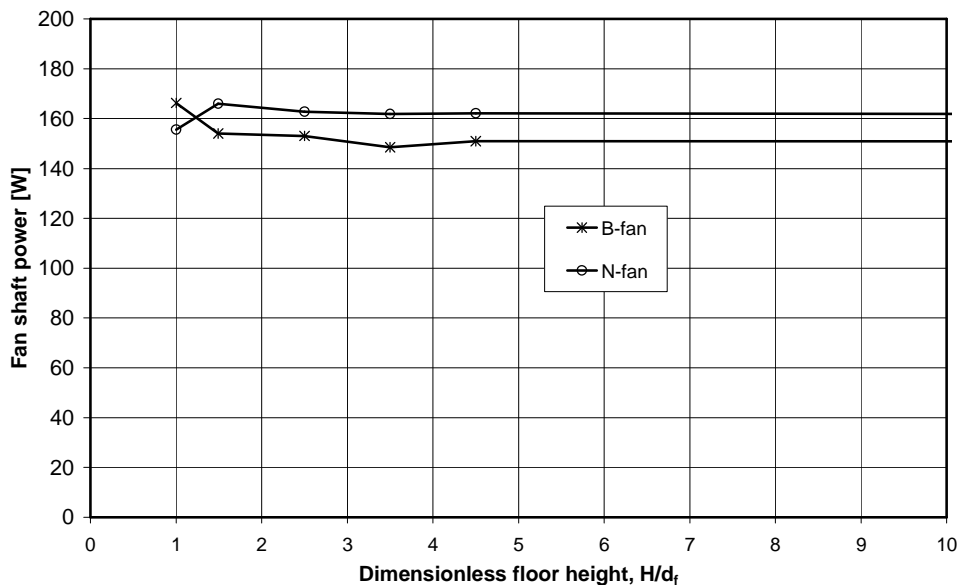


Figure 14: Comparison of fan shaft power.

When considering the fan shaft power consumption in relation to the volumetric effectiveness at the specific operating point of the B- and N-fans, the benefit of the higher efficiency of the B-fan is apparent. Even though the volumetric effectiveness values of the N- and B-fan are similar at large platform heights, the B-fan has a fan shaft power consumption that is 7% lower than that of the N-fan (corresponding to the higher efficiency values shown in Figure 8). At the lowest platform height the shaft power consumption of the B-fan increases and is 6.5% higher than that of the N-fan. This is however still considerably less than the 37.5% greater volumetric effectiveness exhibited by the B-fan at this floor height.

## CONCLUSION

This document presented the single - and multiple fan test results for three different fan designs. It should be emphasized once again that the purpose of the multiple fan tests was not to quantify the effect of floor height on fan volumetric effectiveness but to investigate the performance of the different fan configurations under distorted inlet flow conditions. The following conclusions can be drawn from this investigation:

1. The results from the standard axial flow fan tests prescribed by BS 848 part 1 are applicable to most of the axial flow fans located in an ACSC. However, at large levels of inlet flow distortion, the standard fan test facility no longer represent the operation of an axial flow fan correctly. The volume flow rate through the fan decreases and variations in the shaft power consumption of the fans occur. The multiple fan test facility provides a viable alternative for the standard fan test facility. Practical considerations limit the size of fans that can be tested on this facility and it is recommended that the possibility of quantifying simple distorted inlet condition tests that can be performed on a standard single fan test facility be investigated.
2. As briefly mentioned in the previous section, Van der Spuy<sup>1</sup> used the multiple fan test facility with a set of dummy plenum chambers instead of the flow straighteners used in previous investigations<sup>10</sup>. The possibility of extending the use of the multiple fan test facility to investigate downstream fan installation configurations can therefore be considered.
3. The single fan test results show that higher fan efficiency can be obtained when designing a fan for a specific operating point, like the B-fan, compared to having a single fan design that covers an entire range of operating conditions, like the V-fan. The practical implications of having such a large hub diameter (scaling the B-fan 6 times gives a 3.6 m diameter hub) should however be considered when considering the implementation of the B-fan.
4. The multiple fan test results showed conclusively that a fan with a steeper static pressure characteristic has a higher volumetric effectiveness than a fan with a flatter characteristic when they have the same operating point.
5. When considering the advantage of a possible higher volumetric effectiveness, the fan shaft power being absorbed by a particular fan should always be taken into account. A higher volumetric effectiveness value may lead to increased power plant generator output but if it is achieved by using a fan configuration that has an increased fan shaft power consumption that is more than the increase in power plant output, the net effect would be a reduction in electric power leaving the boundaries of the power plant.

## BIBLIOGRAPHY

- [1] Van der Spuy, S.J. – *Perimeter fan performance in forced draught air-cooled steam condensers*. Ph.D. thesis, Department of Mechanical and Mechatronic Engineering, Stellenbosch University, South Africa, **2011**.
- [2] Van der Spuy, S.J., von Backström, T.W., Kröger D.G. – *Performance of low noise fans in power plant air cooled steam condensers*, Noise Control Engineering Journal, 57 (4), **2009**.
- [3] Venter, S.J. – *The Effectiveness of Axial Flow Fans in A-Frame Plenums*, Ph.D. thesis, Department of Mechanical Engineering, Stellenbosch University, South Africa, **1990**.
- [4] British Standards Institution – Part 1: *Methods for Testing Performance, Fans for General Purposes*, BS 848, **2007**.

- [5] Venter, S.J., Kröger, D.G. – *The effect of tip clearance on the performance of an axial flow fan*, Energy Conversion Management, 33 (2), **1992**.
- [6] Bruneau, P.R.P. – *The Design of a Single Rotor Axial Flow Fan for a Cooling Tower Application*, M.Eng. thesis, Department of Mechanical Engineering, University of Stellenbosch, South Africa, **1994**.
- [7] Louw, F.G., Bruneau, P.R.P., von Backström, T.W., van der Spuy, S.J. – *The design of an axial flow fan for application in large air-cooled heat exchangers*, Submitted to ASME Turbo Expo 2012, Copenhagen, Denmark, **2012**.
- [8] Salta, C.A., Kröger D.G. – *Effect of inlet flow distortions on fan performance in forced draft air-cooled heat exchangers*, Heat Recovery Systems and CHP, 15, **1995**.
- [9] Stinnes, W.H., von Backström, T.W. – *Effect of cross-flow on the performance of air-cooled heat exchanger fans*, Applied Thermal Engineering, 22, **2002**.
- [10] Bredell, J.R., Kröger, D.G., Thiart G.D. – *Numerical Investigation of fan performance in a forced draft air-cooled steam condenser*, Applied Thermal Engineering, 26, **2005**.
- [11] Conradie, P.J.F. – *Edge fan performance in air cooled condensers*, M.Sc.Eng. thesis, Department of Mechanical and Mechatronic Engineering, University of Stellenbosch, South Africa, **2010**.
- [12] Stinnes, W.H. – *The performance of axial fans subjected to forced cross-flow at inlet*, M.Eng. thesis, Department of Mechanical Engineering, University of Stellenbosch, South Africa, **1998**.